VERTICAL RADIATIVE COOLING ENABLED BY REFLECTIVE MIRROR GEOMETRY AND SPECTRALLY SELECTIVE PHYSICAL MODELING

by

Weijie Chen

A Thesis Submitted to the Faculty of the

WYANT COLLEGE OF OPTICAL SCIENCES

In Partial Fulfillment of the Requirements

For the Degree of

M.S. IN OPTICAL SCIENCES

In the Graduate College

THE UNIVERSITY OF ARIZONA

2025

THE UNIVERSITY OF ARIZONA
GRADUATE COLLEGE

As members of the Master's Committee, we certify that we have read the thesis prepared by: Weijie Chen
titled:

and recommend that it be accepted as fulfilling the thesis requirement for the Master's Degree.

Mohamed Elkabbash (Oct 2, 2025 11:58:12 PDT)
Mohamed Elkabbash Date: Oct 2, 2025

Brandon Chalifoux Date: Oct 2, 2025

Leilei Peng Date: Oct 2, 2025

Final approval and acceptance of this thesis is contingent upon the candidate's submission of the final copies of the thesis to the Graduate College.

I hereby certify that I have read this thesis prepared under my direction and recommend that it be accepted as fulfilling the Master's requirement.

Mohamed Elkabbash (Oct 2, 2025 11:58:12 PDT)
Mohamed Elkabbash Date: Oct 2, 2025
Thesis Committee Chair
Wyant College of Optical Sciences

ACKNOWLEDGEMENT

I would like to express my sincere gratitude to my advisor, Prof. Mohamed ElKabbash, for his patient guidance, rigorous academic standards, and unwavering support throughout my graduate studies. His mentorship has been instrumental in shaping my research direction and fostering my growth as a scholar.

I am also thankful to my committee members, Prof. Brandon Chalifoux and Prof. Leilei Peng, for their valuable feedback and thoughtful suggestions during the writing process. Their insights have greatly improved the clarity and depth of this thesis.

Special thanks to Prof. Xuefeng Liu, whose guidance on the writing and structure of this thesis was particularly helpful during the final stages of preparation.

I would also like to sincerely thank my academic advisors, Amber Soergel and Jini Kandyil, for their continuous support and guidance throughout my academic journey—from undergraduate studies to graduate school. Their advice on academic planning, graduate applications, and degree completion has been invaluable.

I am deeply grateful to my family for their constant love and encouragement. In particular, I would like to thank my mother, whose unwavering support and belief in me have been a source of strength throughout this journey.

Although this work did not receive external funding, it has been made possible through the academic and emotional support of those mentioned above. To all who have supported me along the way—thank you.

LAND ACKNOWLEDGEMENT

We respectfully acknowledge the University of Arizona is on the land and territories of Indigenous peoples. Today, Arizona is home to 22 federally recognized tribes, with Tucson being home to the O'odham and the Yaqui. Committed to diversity and inclusion, the University strives to build sustainable relationships with sovereign Native Nations and Indigenous communities through education offerings, partnerships, and community service.

TABLE OF CONTANTS

Abstract
Radiative cooling is a passive cooling method that can reduce electricity use by emitting heat into outer space through the atmospheric transparency window (8–13 μm). Most current designs use horizontal emitters, which are limited by rooftop space in cities. In contrast, vertical surfaces such as building façades are more abundant, but have received little attention due to fundamental physical limitations: they suffer from restricted sky exposure and increased absorption of thermal radiation from the ground and surrounding structures, which significantly reduce net cooling performance when analyzed using conventional models. In this study, we propose a new physical model for vertical radiative cooling, incorporating angular and spectral selectivity as well as geometrical view factor constraints. Based on this model, we design a vertical radiative cooling system that uses angularly and spectrally selective emitters, combined with a reflective mirror placed below the emitter. This design improves the effective emission angle and blocks thermal radiation from the ground. Simulation results show that under typical urban conditions like Phoenix, Arizona, USA (30 °C ambient, atmospheric transmittance $\tau = 0.8$, parasitic heat coefficient $h = 0.8$ W/m²·K), the system can achieve a net cooling power of 16.13 W/m². We also show that with four vertical panels and one horizontal emitter, the system can deliver over 1 kW of total cooling power. Even without rooftop components, a vertical surface area of 62 m² is enough to reach kilowatt-level cooling. These results suggest that vertical radiative cooling is a practical and scalable solution for reducing cooling energy use in dense urban areas, enabled by a physics-based framework tailored to vertical emitter geometry.
Keywords: Radiative Cooling; Atmospheric Transparency Window.

1 Introduction

Cooling systems use nearly 20% of the world's electricity [1]. This number is still rising because of urban growth and global warming. Traditional air conditioning not only needs electricity but also increases carbon emissions. This has created a strong demand for more sustainable cooling methods. One promising solution is passive radiative cooling, which works by emitting heat into outer space through the atmospheric transparency window (8–13 μm), without using any power [2][3].

Most radiative cooling designs use horizontal surfaces, such as rooftops, to emit heat effectively. Based on the ASHRAE residential load example, the typical cooling demand is about 26 W/m^2 [4]. For a standard 60 m^2 room, this corresponds to approximately 1.56 kW of cooling demand. In comparison, the state-of-the-art radiative cooling air conditioner (RC/AC) can provide a net cooling power of about 100 W/m^2 [2][5]. Therefore, cooling a single room would require an RC/AC panel area of at least 15 m^2. However, urban areas often lack sufficient rooftop space, making it difficult to scale up. In contrast, vertical surfaces like building facades are more available, but they have not been utilized for radiative cooling applications.

Using vertical surfaces for radiative cooling introduces two fundamental challenges: the sky view is much more limited, and the surface receives additional upward thermal radiation from the ground, both of which reduce the net cooling power [6]. Xie et al. formalized this with a net-power balance $P_{\text{net}}(T)$ that includes a ground-radiation term unique to vertical emitters, and showed that vertical surfaces must keep absorbed solar power below ~40 W/m^2 to reach sub-

ambient temperatures; they experimentally achieved 2.5±0.7 °C below ambient under > 920 W/m^2 peak sun using an angularly asymmetric spectrally selective emitter [6][7]. Complementary theoretical work demonstrates that combining angular and spectral selectivity is essential to push toward deep subfreezing regimes, but restricting the emission solid angle reduces the emitted power Q_{sample} and thus makes performance highly sensitive to parasitic (conductive/convective) losses; angular selectivity yields a benefit only when such parasitic losses are well managed (e.g., at low effective heat-transfer coefficients), and can otherwise degrade the equilibrium temperature [7][8]. These results highlight why many prior horizontal designs cannot be directly translated to facades and why angular selectivity must be applied with care on vertical emitters [6].

In this work, we consider a vertically oriented thermal emitter where the radiation asymmetry towards the sky is mitigated by using a reflective mirror. We also investigate the effect of angular selectivity, demonstrating how directional control of emission can enhance cooling efficiency. To capture these aspects, we developed a physical model tailored for vertical radiative cooling, which accounts for angular and spectral dependent emission of vertically placed emitters while including geometric view factor limitations and parasitic heat transfer. Based on this model, we design a scalable cooling system that integrate angularly and spectrally selective emitters with a reflective mirror and a vacuum-insulated glass (VIG) thermal barrier [5][9][10]. This configuration enhances the effective emission solid angle, blocks downward thermal input from the ground, and suppresses non-radiative heat gain. Under representative urban conditions in Phoenix, Arizona (ambient temperature = 30 °C, atmospheric transmittance τ = 0.8) [11], the proposed vertical system achieves a net cooling power of 16.13 W/m^2 with wall-mounted emitters. The detailed performance curve as a function of emitter temperature is presented in Fig. 5 (Section 5).

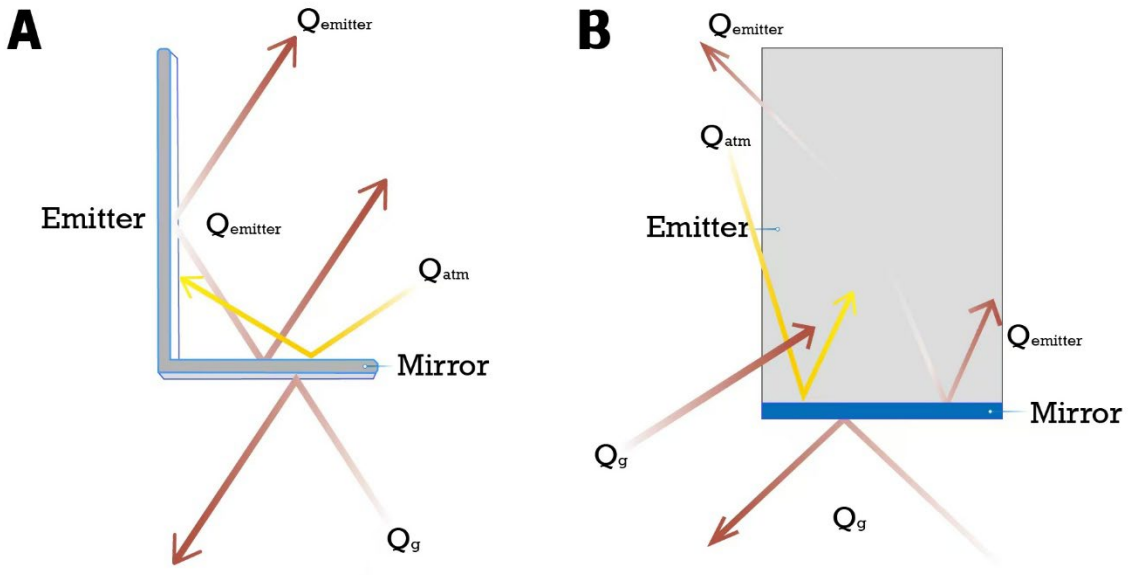

Fig. 1: Schematic of vertical radiative cooling system. (A) Cross sectional view of vertical emitter with a horizontal mirror. (B) Realistic façade mounted emitter and mirror configuration. $Q_{sample}(T)$ ($Q_{emitter}$)is the emitted thermal radiation. $Q_{atm}(T)$ and $Q_g(T)$ are absorbed heat from the atmosphere and the ground. The mirror reflects downward emission and blocks part of ground radiation.

Fig. 1 shows the schematic of the vertical radiative cooling system. In both cases, a vertical emitter is placed above a horizontal reflective mirror. Figure 1A provides a side view in which radiation from the emitter travels upward to the sky as well as downward toward the mirror, which then reflects it upward. The mirror also blocks part of the ground thermal radiation. Figure 1B shows the same configuration from the front view, corresponding to a façade-mounted emitter-mirror system. In this setup, the emitter exchanges radiation with the atmosphere (Q_{sample}), with the ground ($Q_{\mathrm{g}}(T)$), and emits thermal radiation ($Q_{\mathrm{sample}}(T)$). The reflective geometry increases the effective emission solid angle while blocking part of the ground thermal radiation, thereby mitigating parasitic heating.

The following sections explain the physical model of the system and show simulation results under different environmental conditions. These include humidity, parasitic heat loss, and different mirror sizes.

2 Theoretical Background

To analyses the performance of the vertical radiative cooling system, we begin by defining the net heat flux. The total net cooling power of a radiative surface is determined by the balance between emitted radiation and absorbed heat from the environment, including the atmosphere, the ground, and any non-radiative heat exchange. The net radiative heat flux $Q_{\mathrm{net}}(T)$ for a vertical emitter can be expressed as

$$Q_{\mathrm{net}}(T) = Q_{\mathrm{sample}}(T) - Q_{\mathrm{atm}}(T) - Q_{\mathrm{parasitic}}(T)$$

Here, $Q_{\mathrm{sample}}(T)$ is the emitted radiative heat flux from the vertical surface. $Q_{\mathrm{atm}}(T)$ and $Q_{\mathrm{g}}(T)$ are the absorbed infrared radiation from the atmosphere and the ground, respectively. $Q_{\mathrm{parasitic}}(T)$ represents parasitic heat input from conduction and convection, which is not related to radiation. The value of $Q_{\mathrm{net}}(T)$ depends on emitter temperature, material properties, geometry and surrounding conditions.

In this section, we describe how our proposed geometry, using a vertical emitter combined with a reflective mirror, modifies these components and improves radiative cooling performance under realistic conditions.

2.1 The heat flux from vertical emitter with reflective mirror

To evaluate the total emitted power from the vertical surface, we start by analyzing a basic case without any mirror. In this case, the heat flux emitted from the emitter surface is given by:

$$Q_{\mathrm{sample}}(T) = \int_0^{\pi} d\varphi \int_0^{\frac{\pi}{2}} d\theta \sin\theta \cos\theta \int_0^{\infty} d\lambda \, I_{\mathrm{BB}}(T,\lambda)\varepsilon(\lambda,\theta)$$

Here, φ and θ are the azimuthal and zenith angles of thermal emission. For a vertical emitter, thermal radiation emitted at angles $\theta < \pi/2$ can reach the sky and contribute to cooling, while radiation emitted toward the ground ($\theta > \pi/2$) does not. Since the emitter surface is flat, the azimuthal angle varies from 0 to π. The double integral over φ and θ defines the solid angle through which useful emission occurs.

In the equation, $I_{BB}(T,\lambda) = \frac{2hc^2}{\lambda^5}\frac{1}{e^{\frac{hc}{\lambda k_B T}}-1}$ is the blackbody spectral intensity at temperature T, where h is Planck's constant, c is the speed of light, k_B is the Boltzmann constant, and λ is the wavelength. The emissivity $\varepsilon(\lambda,\theta)$ depends on both the emission wavelength and angle.

Introducing a reflective mirror beneath the vertical emitter increases the effective solid angle for thermal radiation to escape to the sky. The mirror reflects some of the downward emission upward and blocks part of the ground radiation. To quantify this enhancement, we define the maximum zenith angle θ_m and azimuthal angle φ_m for reflected radiation that can reach the sky. These angles depend on the geometry between the emitter and the mirror.
Assum the vertical emitter has a surface of length L_e and width W_e, and the mirror has length L_m and width W_m. The angular limits of reflected emission form the mirror toward the sky can be expressed as (see Appendix B for derivation):

$$\theta_m = \tan^{-1}\left(\frac{L_m}{\sqrt{\left(\frac{L_e}{2}\right)^2 + \left(\frac{W_m}{4}\right)^2}}\right)$$

$$\varphi_m = 2 \times \tan^{-1}\left(\frac{W_m 2}{\sqrt{\left(\frac{L_e}{2}\right)^2 + \left(\frac{L_m}{2}\right)^2}}\right)$$

Accordingly, the additional heat flux emitted due to the mirror reflection is denoted as $Q_{\text{sample,m}}(T)$. This contribution covers the range of reflected angles defined by θ_m and φ_m, as derived above. It is calculated by:

$$Q_{\text{sample,m}}(T) = \int_0^{\varphi_m} d\varphi \int_0^{\theta_m} d\theta \sin\theta \cos\theta \int_0^{\infty} d\lambda \, I_{\text{BB}}(T,\lambda)\varepsilon(\lambda,\theta)$$

This expression has the same form as the original direct emission $Q_{\text{sample}}(T)$, but the integration rage is extended due to the mirror reflection. Therefore, the total emitted heat flux from the vertical emitter with the mirror is:

$$Q_{\text{sample,total}}(T) = Q_{\text{sample}}(T) + Q_{\text{sample,m}}(T)$$

This total value represents the full radiative cooling contribution from both direct emission and mirror-enhanced reflected emission. In the next section, we evaluate the atmospheric and ground radiation absorbed by the emitter.

2.2 The atmospheric thermal radiation absorbed by emitter

The atmospheric thermal radiation absorbed by the emitter is denoted as $Q_{\mathrm{atm}}(T_{\mathrm{atm}})$, where T_{atm} is the ambient air temperature (assumed to be 300K). The absorbed heat flux is calculated by integrating over the upper hemisphere:

$$Q_{\mathrm{atm}}(T_{\mathrm{atm}}) = \int_0^{\pi} d\varphi \int_0^{\frac{\pi}{2}} d\theta \sin\theta \cos\theta \int_0^{\infty} d\lambda \, I_{\mathrm{BB}}(T_{\mathrm{atm}}, \lambda)\varepsilon(\lambda, \theta)\varepsilon_{\mathrm{atm}}(\lambda, \theta)$$

Here, $\varepsilon_{\mathrm{atm}}(\lambda, \theta)$ is the directional emissivity of the atmosphere, defined as: $\varepsilon_{\mathrm{atm}}(\lambda, \theta) = 1 - \tau_{\mathrm{atm}}^{\frac{1}{\cos\theta}}$, where τ_{atm}~0.8 represents the average transmittance in the mid-infrared atmospheric window (8-13 μm), and θ is the polar angle [8]. Outside this range, $\varepsilon_{\mathrm{atm}}$ is assumed to be zero for simplicity. The term $I_{\mathrm{BB}}(T_{\mathrm{atm}}, \lambda)$ is the blackbody intensity at atmospheric temperature.

In addition to direct radiation from the sky the reflective mirror increases the amount of atmospheric heat absorbed by reflecting some radiation from lower angles. This contribution, denoted as $Q_{\mathrm{atm,m}}(T_{\mathrm{atm}})$, is calculated over the same angular limits used for the mirror-enhanced emission:

$$Q_{\mathrm{atm,m}}(T_{\mathrm{atm}}) = \int_0^{\varphi_m} d\varphi \int_0^{\theta_m} d\theta \sin\theta \cos\theta \int_0^{\infty} d\lambda \, I_{\mathrm{BB}}(T_{\mathrm{atm}}, \lambda)\varepsilon(\lambda, \theta)\varepsilon_{\mathrm{atm}}(\lambda, \theta)$$

Thus, the total atmospheric radiation absorbed by the emitter is:

$$Q_{\mathrm{atm,total}}(T_{\mathrm{atm}}) = Q_{\mathrm{atm,m}}(T_{\mathrm{atm}}) + Q_{\mathrm{atm}}(T_{\mathrm{atm}})$$

This total accounts for both the direct atmospheric absorption and the extra contribution caused by mirror reflection.

2.3 The infrared radiation from the ground

The vertical emitter also absorbs infrared radiation from the ground. This heat flux, denoted as $Q_{\mathrm{g}}(T_{\mathrm{g}})$, is calculated over the lower hemisphere, where T_{g} is the ground temperature (assumed here as 300K). The integral form is:

$$Q_{\mathrm{g}}(T_{\mathrm{g}}) = \int_0^{\pi} d\varphi \int_{\frac{\pi}{2}}^{\pi} d\theta \sin\theta \cos\theta \int_0^{\infty} d\lambda \, I_{\mathrm{BB}}(T_{\mathrm{g}}, \lambda)\varepsilon(\lambda, \theta)\varepsilon_{\mathrm{g}}$$

Here, the zenith angle θ range from $\pi/2$ to π, corresponding to radiation arriving from below. Natural surfaces such as soil, concrete, and vegetation are typically diffuse emitters with weal angular dependence. Therefore, we assume the ground emissivity ε_{g} is constant at 0.9.

In systems using a mirror, part of the ground radiation is blocked from reaching the emitter. The portion of radiation blocked by the mirror is denoted as $Q_{\mathrm{g,m}}(T_{\mathrm{g}})$, and is calculated using the mirror-reflection angles θ_m and φ_m:

$$Q_{\mathrm{g,m}}(T_{\mathrm{g}}) = \int_0^{\varphi_m} d\varphi \int_0^{\theta_m} d\theta \sin\theta \cos\theta \int_0^{\infty} d\lambda \, I_{\mathrm{BB}}(T_{\mathrm{g}}, \lambda)\varepsilon(\lambda, \theta)\varepsilon_{\mathrm{g}}$$

This term represents the radiation that would otherwise reach the emitter but is reflected away or blocked by the mirror. The net absorbed ground radiation is then given by:

$$Q_{\mathrm{g,total}}(T_{\mathrm{g}}) = Q_{\mathrm{g,m}}(T_{\mathrm{g}}) + Q_{\mathrm{g}}(T_{\mathrm{g}})$$

This total accounts for the full contribution of ground thermal radiation minus the portion prevented by the mirror.

2.4 The parasitic heat flux

In addition to radiative processes, the emitter also experiences non-radiative heat input from its environment. This parasitic heat flux, denoted as $Q_{\mathrm{parasitic}}(T, T_{\mathrm{amb}})$, includes both conduction and convection, and is modeled as:

$$Q_{\mathrm{parasitic}}(T, T_{\mathrm{amb}}) = h(T_{\mathrm{amb}} - T)$$

Here, $h = h_{\mathrm{cond}} + h_{\mathrm{conv}}$ is the total non-radiative heat transfer coefficient. It accounts for heat exchanged between the emitter and surrounding air or supporting structures through physical contact and natural convection.

2.5 The net cooling power

With all contributions considered, the total net cooling power of the vertical emitter is:

$$\begin{aligned} Q_{\mathrm{net}}(T) = {} & Q_{\mathrm{sample}}(T) + Q_{\mathrm{sample,m}}(T) \\ & -\left[Q_{\mathrm{atm}}(T) + Q_{\mathrm{atm,m}}(T) + Q_{\mathrm{g}}(T) - Q_{\mathrm{g,m}}(T) + Q_{\mathrm{parasitic}}(T, T_{\mathrm{amb}})\right] \end{aligned}$$

This equation captures all radiative and non-radiative energy exchanges. Positive Q_{net} values correspond to cooling performance, while negative values indicate net heating.

Spectral and angular selectivity further improve cooling efficiency. Spectral selectivity restricts thermal emission to the 8 – 13μm atmospheric widow, while angular selectivity limits radiation to directions that avoid ground absorption and atmospheric back-emission. These principles are implemented in our design and discussed in detail in Appendix B.

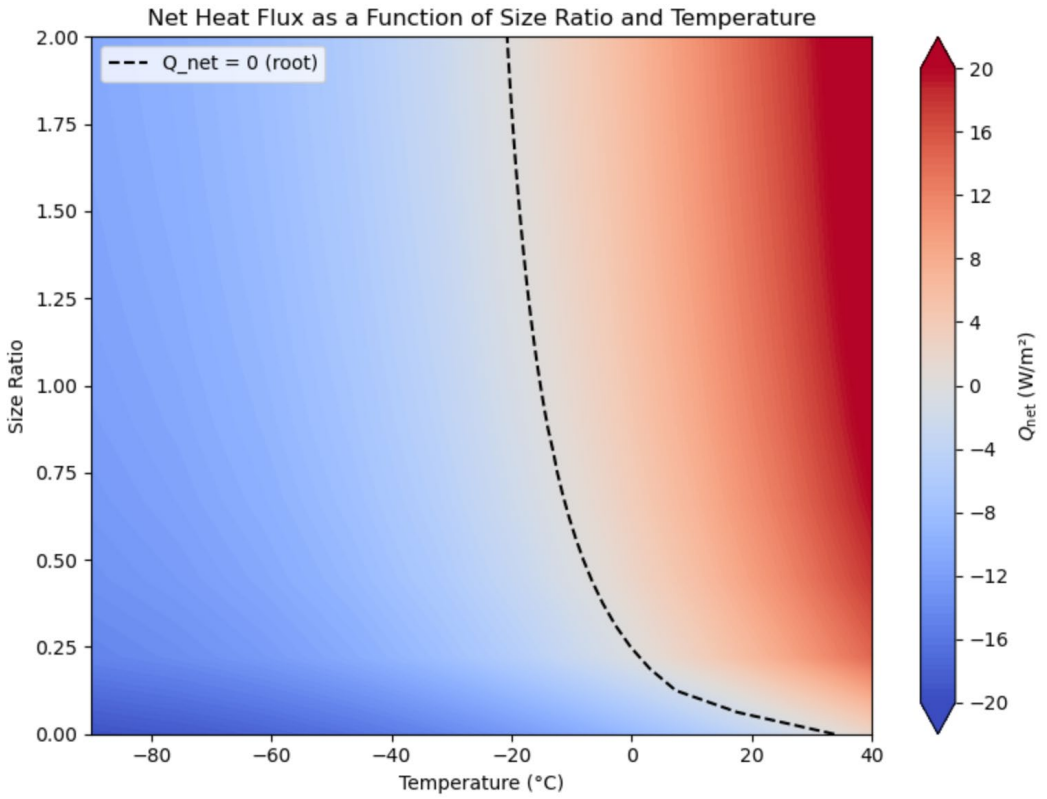

Fig. 2: Simulated net radiative heat flux Q_{net} as a function of emitter temperature and mirror-to-emitter area ratio. The black dashed contour indicates the condition $Q_{net} = 0$, which corresponds to the balance temperature.

Fig. 2 shows the effect of mirror-to-emitter size ratio on the net radiative heat flux $Q_{\text{net}}(T)$. The size ratio is defined as the total mirror area divided by the emitter area. Increasing this ratio improves cooling performance by expanding the effective emission angle and reducing ground radiation.

The color map shows that as the mirror-to-emitter ratio increases, the emitter reaches a lower equilibrium temperature, indicated by the $Q_{\text{net}} = 0$ contour. When the ratio reaches approximately 1, the system can achieve subfreezing operation with a balance temperature around -20 °C. Beyond this point, additional mirror area only yields small gains, while increasing fabrication complexity, Therefore, a ratio of 1 is selected for all subsequent analysis.

3 Effect of Atmospheric Water Vapor

Atmospheric water vapor strongly affects radiative cooling because it absorbs infrared radiation outside the 8-13 μm atmospheric window, thereby reducing the transmittance of thermal emission to space [12][13]. Lower values of τ_{atm} correspond to higher water vapor content and thus result in reduced cooling power. The atmospheric transmittance is related to precipitable water (PW), which measures the depth of water vapor in the atmospheric column. PW can vary from less than 5 mm in arid regions to over 50 mm in humid tropical climates, corresponding to a wide range of τ_{atm} value.

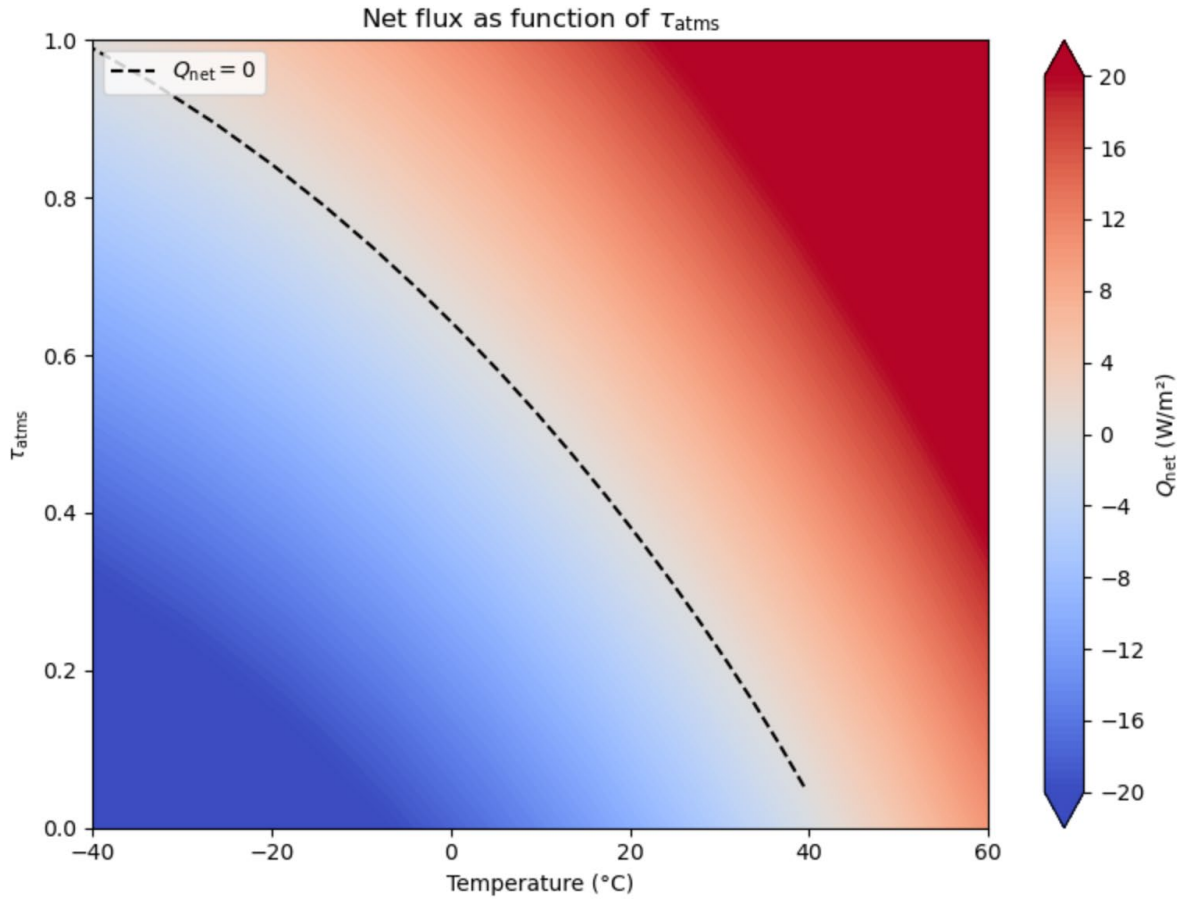

Fig. 3: Simulated net radiative heat flux Q_{net} as a function of emitter temperature and atmospheric transmittance τ_{atm}, under angularly and spectrally selective conditions. The dashed contour indicates the condition $Q_{net} = 0$, corresponding to the equilibrium temperature of the emitter.

To quantify this effect, Fig. 3 shows the influence of atmospheric transmittance τ_{atm} on the cooling performance of the proposed vertical emitter. The simulation assumes a spectrally selective emitter, angular selectivity limited to 30°, a mirror-to-emitter area ratio of 1, and no parasitic heat loss ($Q_{\mathrm{parasitic}} = 0$). The black contour represents the condition where emission balance absorbed atmospheric and ground radiation ($Q_{\mathrm{net}} = 0$), which corresponds to the balance temperature of the emitter.

The results demonstrate that cooling performance improves as τ_{atm} increases. Notably, even when $\tau_{\mathrm{atm}} > 0.65$, which corresponds to moderate humidity levels, the system still maintains net radiative cooling. This suggests that the proposed vertical cooling design is robust and can operate effectively in diverse climate conditions, including areas with higher atmospheric moisture.

4 Effect of Parasitic Heating

In real-world applications, the performance of radiative cooling systems is often limited by non-radiative heat gain from the surroundings. This unwanted heat input, known as parasitic heating, results from both conduction and convection between the emitter surface and ambient air or

support structures. If not controlled, parasitic heat can significantly reduce the net cooling power and prevent the system from achieving sub-ambient or subfreezing temperatures.

Fig. 4 shows the simulated net heat flux Q_{net} as a function of emitter temperature and the parasitic heat transfer coefficient $h_{\text{parasitic}}$. The simulation assumes a spectrally and angularly selective emitter (30° limit), a mirror-to-emitter area ratio of 1, and an atmospheric transmittance of $\tau_{\text{atm}} = 0.8$, without considering humidity or wind. The results indicate that when $h_{\text{parasitic}}$ is below approximately 2 $\text{W}\cdot\text{m}^{-2}\cdot\text{K}^{-1}$, strong sub-ambient cooling is achievable across a wide temperature range. However, as $h_{\text{parasitic}}$ increases beyond this value, the cooling window narrows rapidly. For example, when $h_{\text{parasitic}} > 4\ \text{W}\cdot\text{m}^{-2}\cdot\text{K}^{-1}$, the emitter temperature must stay very close to ambient to maintain cooling and further increases in h result in complete loss of cooling ability.

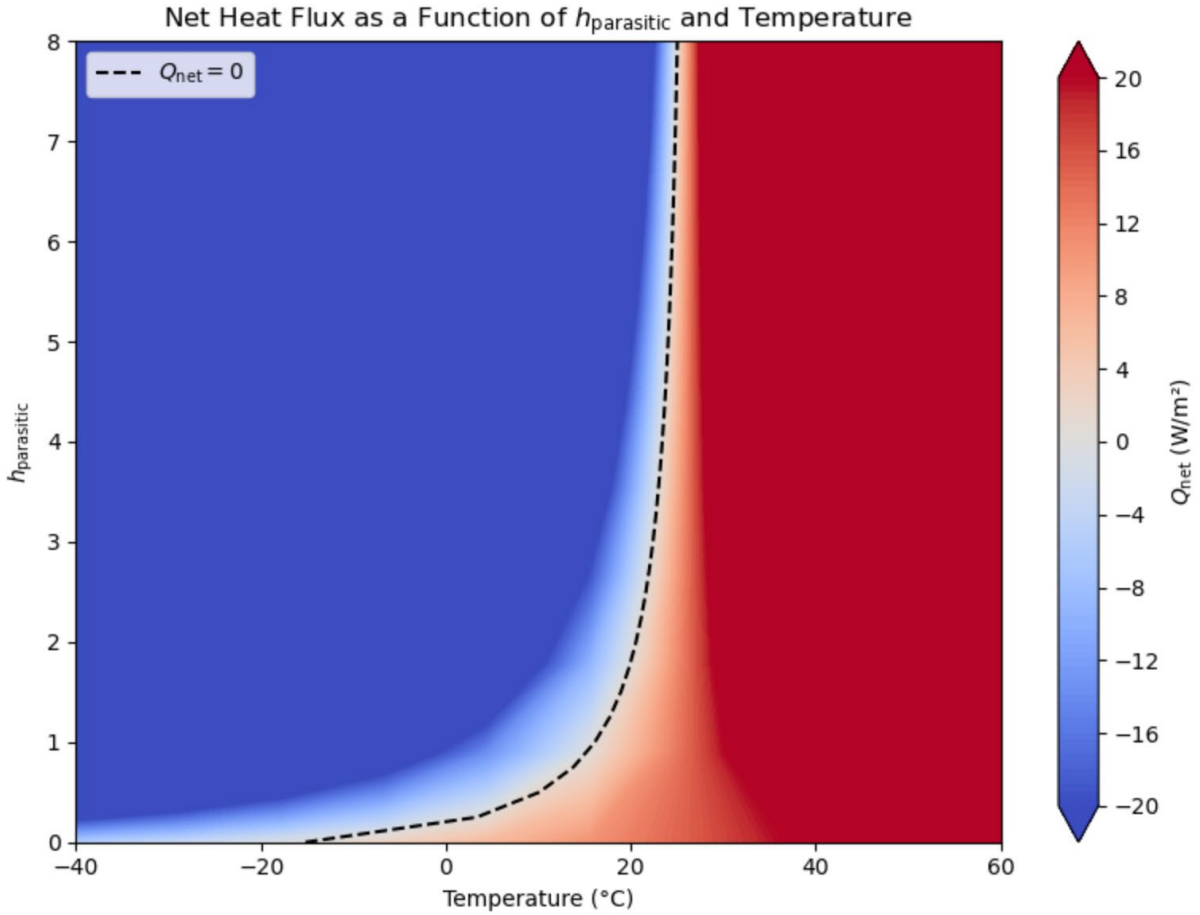

Fig. 4: Simulated net radiative heat flux Q_{net} as a function of emitter temperature and parasitic heat transfer coefficient $h_{parasitic}$. The dashed line indicates the condition $Q_{net} = 0$, representing the balance temperature.

It is important to note that the introduction of angularly selective thermal emission, although highly effective in mitigating atmospheric radiative input, inherently reduces the total emitted radiation power to outer space. As a result, the system becomes more vulnerable to parasitic heating, since even a modest amount of non-radiative heat gain can outweigh the reduced radiative cooling capacity. This effect has been highlighted in previous work, where the combination

of selective emission and environmental parasitic heating was shown to limit the achievable sub-ambient cooling performance [14]. Therefore, when integrating angular selectivity into vertical radiative cooling systems, addressing parasitic heating through thermal insulation strategies is particularly critical.

To suppress parasitic heat transfer in practice, we propose the use of vacuum insulated glass (VIG) in contact with the emitter surface. VIG eliminates convective and gaseous conductive heat flow through a vacuum gap, forming an effective thermal barrier. According to Simko et al., VIG can achieve a thermal conductivity as low as 0.8 $W \cdot m^{-2} \cdot K^{-1}$. This allows subfreezing radiative cooling even under non-laboratory conditions. Therefore, combining angular and spectral selectivity with passive insulation structures such as VIG can significantly enhance the practical performance of vertical radiative cooling systems.

However, conventional VIG uses soda-lime or borosilicate glass, which is opaque in the mid-infrared range. These materials block thermal emission in the 8-13 μm atmospheric transparency window, thereby limiting radiative cooling performance. To address this limitation, we propose replacing the standard VIG glass with barium fluoride (BaF_2), which exhibits high transmittance (>90%) across the 8-13 μm band, allowing thermal radiation to effectively escape to outer space.

Although BaF_2 is mechanically softer and hygroscopic, these issues can be mitigated in our design. The emitter is supported by a micro-pillar VIG structure, which provides mechanical stability while maintaining a vacuum gap to eliminate non-radiative losses. To protect BaF_2 from moisture degradation and improve optical performance, a thin magnesium fluoride (MgF_2) coating is applied to its outer surface. MgF_2 serves both as a moisture barrier and anti-reflection (AR) coating, further enhancing infrared transmittance.

This integrated design, combining BaF_2 window material, MgF_2 functional coating, and micro-structured VIG thermal insulation, preserves the advantages of radiative cooling through the atmospheric window, minimizes parasitic heat gain, and ensures structural robustness. When used in conjunction with angular and spectral selectivity as well as reflective mirror enhancement, this architecture enables practical and scalable implementation of high-performance vertical radiative cooling devices.

5 Realistic Design under Urban Conditions

To assess the practical performance of our proposed vertical radiative cooling system, we conducted simulations based on the environmental conditions of Phoenix, Arizona, a hot and arid city with a typical summer daytime ambient temperature of approximately 30 °C and annual precipitation of 183 mm [11]. This corresponds to an estimated mid-infrared atmospheric transmittance of $\tau_{\mathrm{atm}} \approx 0.8$, based on established relationships between precipitable water and spectral transparency [2].

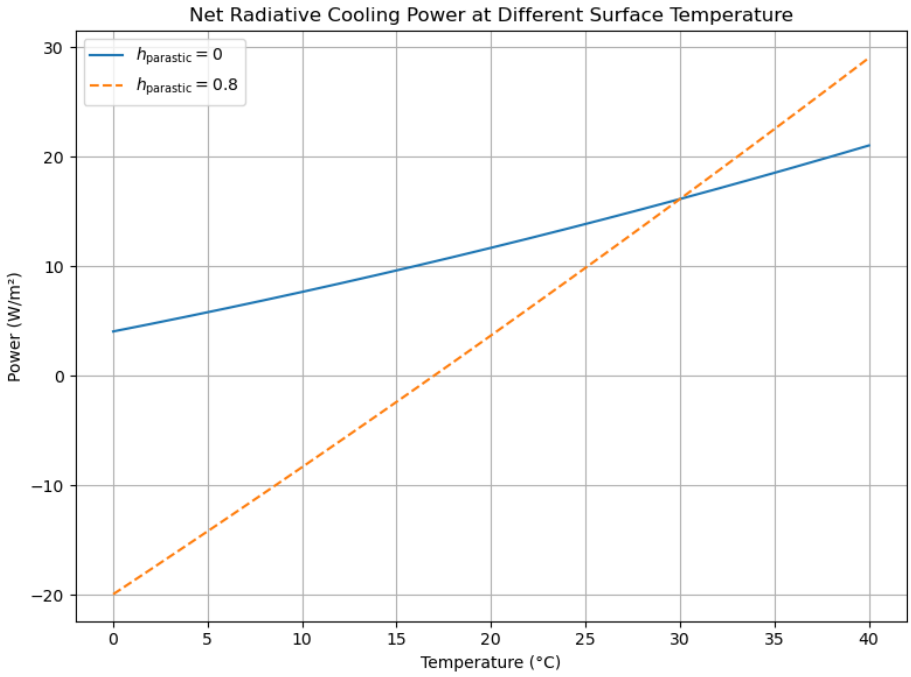

Fig. 5: Net radiative cooling power vs. emitter temperature in Phoenix, AX (T = 30 °C, τ = 0.8). Blue line shows ideal case (no parasitic heat), orange dashed line shows case with vacuum insulated glass (h = 0.8 W/m2). The system reaches 16.13 W/m2 of cooling power at 30 °C.

Under these conditions, our vertical cooling system, featuring a BaF_2 window material for mid-infrared transparency, a MgF_2 functional coating for moisture protection and anti-reflection, and a VIG-based micro-pillar structure for thermal insulation, achieves a net radiative cooling power of approximately 16.13 W/m^2 at 30 °C. As shown in Fig. 5, this performance is sustained despite non-radiative heat losses ($h_{\text{parasitic}} = 0.8\ \text{W} \cdot \text{m}^{-2} \cdot \text{K}^{-1}$), a value consistent with vacuum insulated glazing (VIG) structures reported in the Simko's work [10]. This demonstrates the feasibility of vertical radiative cooling in realistic urban environments.

To illustrate potential deployment, we consider a rectangular water tank enclosed by four vertical cooling panels (each 10 m^2) and one horizontal emitter on the top surface. The horizontal emitter, assumed to be spectrally selective, provides a peak cooling power of ~40 W/m^2 based on previous experimental data [5]. The four vertical panels contribute:$4 \times 10\ \text{m}^2 \times 16.14\ \text{W/m}^2 = 645.2$ W. Combining vertical and horizontal contributions yields a total cooling capacity of approximately 10045 W under typical Phoenix summer conditions.

Alternatively, even without any horizontal surface, the system can still provide over 1kW of cooling using only vertical emitters. A total vertical area of approximately 62 m^2 operating at 16.13 W/m^2 would be sufficient. This requirement is feasible for building façades, which often offer large unused wall surfaces. Therefore, the proposed design provides a scalable and practical solution for integrating radiative cooling into urban environments, especially where rooftop space is limited.

6 Conclusion

In this study, we present a vertical radiative cooling system designed to operate effectively under direct sunlight and realistic urban conditions. By combining angularly and spectrally selective emitters with a reflective mirror and an integrated thermal insulation structure, the design addresses key limitations of conventional horizontal radiative coolers – particularly in dense cities with limited rooftop space.

Our approach introduces several innovations. The use of a reflective mirror enhances the effective emission solid angle while reducing ground radiation absorption. The emitter structure integrates a BaF_2 window material, which provides high transmittance in the 8-13 μm infrared band, and an MgF_2 coating for moisture protection and anti-reflection. These are supported by a vacuum-insulated micro-pillar (VIG) base, which minimizes parasitic heat gain without compromising structural integrity.

Through theoretical modeling and simulation, we demonstrate that the proposed system achieves a net cooling power of 16.13 W/m^2 under ambient conditions representative of Phoenix, Arizona (30 °C, $\tau = 0.8$, $h = 0.8$ $W \cdot m^{-2} \cdot K^{-1}$). This performance enables kilowatt-scale cooling using only vertical surfaces, a target that previously required large horizontal collectors. Even without any rooftop components, a vertical area of 62 m^2 is sufficient to achieve over 1 kW of passive cooling, making this approach feasible for integration into existing building façades.

These results confirm that vertical radiative cooling is not only physically viable but also architecturally scalable. This platform opens new opportunities for sustainable urban thermal management, especially in hot and space-constrained environments. Future work may focus on experimental prototyping, long-term material stability under outdoor exposure, and integration with hybrid passive-active cooling system for year-round energy saving.

Appendix A: Design Principles and Advantages of Angularly Selective Thin-Film Thermal Emitters

In this appendix, we provide additional background and design rationale for angularly selective thermal emitters, which are a critical component of the vertical radiative cooling system proposed in this study. While the main text introduces the use of angular and spectral selectivity in improving cooling performance, the theoretical basis and structural realization of angularly selective emitters are elaborated here.

A.1 Physical Principle of Angular Selectivity

Angular selectivity refers to the directional dependence of a material's emissivity $\varepsilon(\lambda, \theta)$, where λ is the wavelength and θ is the emission angle. The motivation for angular selectivity arises from the angular variation of atmospheric emissivity $\varepsilon_{atm}(\lambda, \theta)$, which increases with emission angular due to the increasing path length through the atmosphere. As a result, thermal radiation emitted at large angles is more likely to be reabsorbed by the atmosphere.

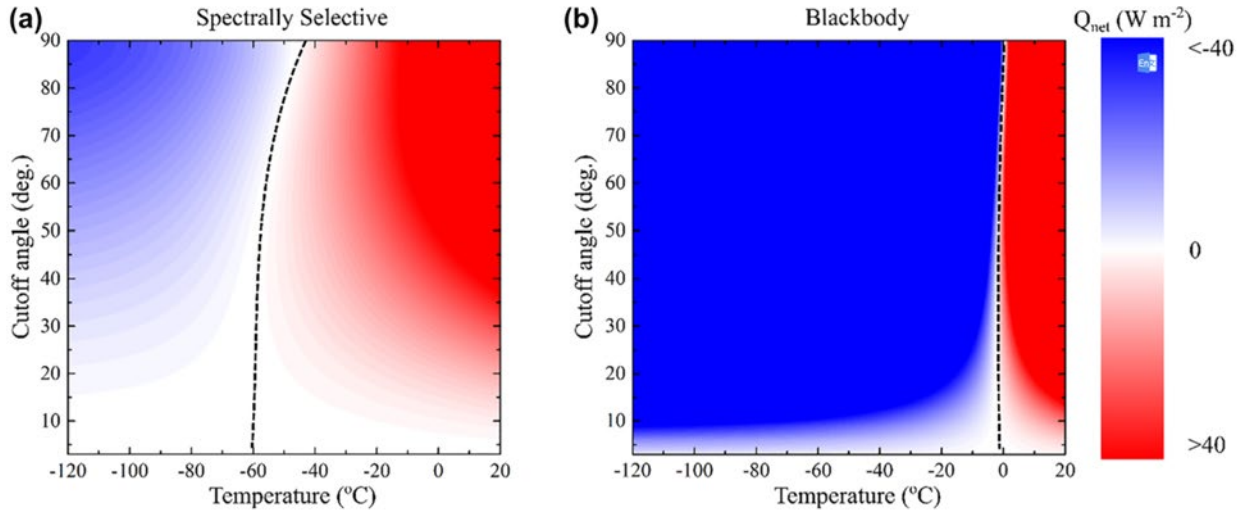

Fig. 6: Effect of angular selectivity on net radiative cooling performance. (a) Spectrally selective emitter with angular restriction. (b) Blackbody emitter without angular restriction. Contour maps show Q_{net} as function of emission temperature and cutoff angle. Dashed lines indicate $Q_{net} = 0$. Adapted from Chamoli et al., Nanophotonics, 2022 [7].

To enhance net radiative cooling and suppress atmospheric back-radiation, it is advantageous to restrict emission to smaller zenith angles. This strategy is especially beneficial in humid environments where $\varepsilon_{\mathrm{atm}}$ is generally high at all wavelengths, particularly in the 8-13 μm infrared window.

Fig. 6a illustrates the effect of angular selectivity on net cooling performance under idealized conditions. A spectrally selective emitter with angular restriction (Fig. 6a) maintains significantly lower equilibrium temperature compared to a blackbody emitter (Fig. 6b) due to reduced atmospheric absorption at low angles. These results demonstrate that angular selectivity provides an additional degree of control in radiative cooling design, complementing spectral selectivity.

A.2 Thin-Film Implementation

Chamoli et al. (2022) proposed a practical thin-film architecture for realizing angularly selective thermal emission. Their design consists of:

A spectrally selective thermal emitter made of 0.8 μm Si_3N_4, which exhibits strong absorption in the 8-23 μm atmospheric window.

A Fabry-Perot transmission filter formed by alternating BaF_2 and LiF layers. These layers act as dielectric mirrors, providing high angular dependence in the mid-infrared.

A ZnS substrate, chosen for its mechanical robustness and high infrared transmittance.

This multilayer stack provides near-unity emissivity at normal incidence and strongly suppresses emission beyond a cutoff angle of ~50°. The total thickness of the structure is only ~16 μm and consists of 10 layers, significantly reducing the fabrication complexity compared to previously proposed photonic crystal designs.

A.3 Performance Advantage

Theoretical modeling indicates that under ideal conditions (no parasitic heat loss), this emitter design can achieve equilibrium temperatures up to 60 °C below ambient. Even under parasitic heat transfer of 8 $W \cdot m^{-2} \cdot K^{-1}$, the temperature from remains around 5 °C. Compared to omnidirectional emitters, this performance enhancement is substantial.

Angular selectivity is particularly valuable in urban environments or high-humidity conditions, where atmospheric emissivity is elevated and lateral ground reflections are common. Combined with spectral selectivity and reflective mirror geometry, this design supports high-efficiency radiative cooling using vertical surfaces.

A.4 Relevance to this Work

In this thesis, the proposed vertical radiative cooling system leverages angular and spectral selectivity to minimize undesired heat gain and maximize net radiative power. While the main text discusses angular limits and mirror-induced enhancements, the material implementation of angle-restricted emission complements this geometric approach. The insights from Chamoli et al. provide a feasible path to fabricating practical angularly selective coatings compatible with vertical deployment.

Appendix B: Derivation of Effective Emission Angle

To understand the enhancement in effective thermal emission caused by the reflective mirror in the vertical emitter configuration, we derive the expressions for the maximum zenith angle (θ_m) and azimuthal angle (φ_m) of radiation reflected toward the sky [15].

B.1 System Geometry

We consider a vertical emitter of length L_e and witdthe W_e, with a reflective mirror of length L_m and width W_m positioned horizontally below the emitter at ground level.

Thermal radiation emitted downward from the vertical surface can be reflected by the mirror into the upward hemisphere, effectively increasing the solid angle through which the emitter radiates to the sky.

We define:
θ_m: Maximum effective zenith angle (in the emitter-mirror-sky plane).
φ_m: Maximum effective azimuthal angle (perpendicular to the above plane).

To derive these angles, we consider the furthest point on the mirror contributing to reflected emission reaching the atmosphere.

B.2 Zenith Angle Derivation (θ_m)

We analyze a vertical cross-sectional plane containing the emitter and the mirror. From simple geometry, the maximum zenith angle is defined as the angle between the vertical line through the emitter and the line connecting the emitter edge to the farthest effective reflection point on the mirror.

Let:

- The vertical distance from the emitter to the effective mirror edge be $d_1 = \sqrt{(L_e/2)^2 + (W_m/4)^2}$
- The horizontal distance is the mirror height L_m.

Then:

$$\theta_m = \tan^{-1}\left(\frac{L_m}{\sqrt{(L_e/2)^2 + (W_m/4)^2}}\right)$$

B.3 Azimuthal Angle Derivation (φ_m)

In the perpendicular plane (top view), we analyze the effective widening of the azimuthal spread caused by mirror reflections.

The horizontal half-width of the mirror is $W_m/2$, and the effective diagonal distance to the far edge is:

$$d_2 = \sqrt{(L_e/2)^2 + (L_m/2)^2}$$

Therefore, the effective half-azimuthal angle is:

$$\varphi_m/2 = \tan^{-1}\left(\frac{W_m/2}{\sqrt{(L_e/2)^2 + (L_m/2)^2}}\right)$$

So the full azimuthal angle is:

$$\varphi_m = 2 \times \tan^{-1}\left(\frac{W_m/2}{\sqrt{(L_e/2)^2 + (L_m/2)^2}}\right)$$

B.4 Physical Interpretation

These expressions approximate the angular limits within which reflected thermal radiation can effectively escape to the sky. When computing the net radiative heat flux, the integrals over solid angle should use these bounds instead of the narrower limits from the bare vertical configuration. This significantly enhances the effective emission angle, enabling stronger radiative cooling.

B.5 Assumptions and Notes

Atmospheric refraction and Earth's curvature are neglected.
Mirror is assumed to be ideal and specular with no absorption.
Geometry is symmetrical around the vertical emitter.
Only first-order reflection is considered (no multiple reflections or scattering).

Appendix C: Simulation Methodology

This study employs custom Python scripts to simulate the radiative het exchange and thermal equilibrium of a vertical selective emitter under different environmental conditions. The simulations are based on numerical integration of directional and spectral radiative heat fluxes. The simulations are based on numerical integration of directional and spectral radiative heat fluxes. The methodology includes the following components:

C1 Radiative Model

The net radiative power is calculated by integrating spectral blackbody radiation, modulated by the emitter's angular-spectral emissivity, atmospheric transmittance, and view factors involving the mirror geometry (see Fig. 2 for schematic). Emissivity is assumed to be unity within the 8-13 μm band and zero elsewhere.

C2 Mirror-Angle Solid Angle Calculation

The view angle of the mirror is converted into solid angle via analytic geometry, as described in Appendix B.

C3 Simulation Variables

Three main environmental or system parameters were varied in the simulations:

- Mirror-to-emitter size ratio
- Atmospheric transmittance (τ_{atm}) over the 8-13 μm band
- Parasitic heat transfer coefficient ($h_{\mathrm{parasitic}}$)

C4 Steady-State Temperature Computation

For each configuration, the equilibrium temperature is found by solving $Q_{\mathrm{net}}(T) = 0$ using Brent's root-finding method, with a temperature range from -100 °C to 40 °C.

C5 Tools and Libraries

The simulation employs Python 3.8 with the NumPy, SciPy, and Matplotlib libraries. The scipy.integrate,dblquad function is used for evaluating double integrals over angle and wavelength space. Each script outputs plots such as temperature-power curves and cooling performance maps under varying design conditions.

Reference

[1] IEA, *The Future of Cooling*, IEA, Paris (2018).

[2] A. P. Raman, M. A. Anoma, L. Zhu, E. Rephaeli, and S. Fan, "Passive radiative cooling below ambient air temperature under direct sunlight," *Nature* **515**, 540–544 (2014).

[3] E. Rephaeli, A. Raman, and S. Fan, "Ultrabroadband photonic structures to achieve high-performance daytime radiative cooling," *Nano Lett.* **13**(4), 1457–1461 (2013).

[4] ASHRAE, *ASHRAE Handbook – Fundamentals, Chapter 17: Residential Cooling and Heating Load Calculations*, American Society of Heating, Refrigerating and Air-Conditioning Engineers, Atlanta, GA (2017).

[5] Y. Zhai, Y. Ma, S. N. David, D. Zhao, R. Lou, G. Tan, … and X. Yin, "Scalable-manufactured randomized glass-polymer hybrid metamaterial for daytime radiative cooling," *Science* **355**(6329), 1062–1066 (2017).

[6] Y. Xie, J. Li, S. He, Y. Liu, S. Liu, L. Xu, … and Q. Zhang, "Subambient daytime radiative cooling of vertical surfaces," *Science* **384**(6692), 436–441 (2024).

[7] S. K. Chamoli, W. Li, C. Guo, and M. ElKabbash, "Angularly selective thermal emitters for deep subfreezing daytime radiative cooling," *Nanophotonics* **11**(16), 3709–3717 (2022).

[8] Z. Chen, L. Zhu, A. Raman, and S. Fan, "Radiative cooling to deep subfreezing temperatures through a 24-h day-night cycle," *Nat. Commun.* **7**, 1–5 (2016).

[9] T. M. Simko, A. H. Elmahdy, and R. E. Collins, "Determination of the overall heat transmission coefficient (U-Value) of vacuum glazing," *ASHRAE Trans.* **105**(2), 1–9 (1999).

[10] Simko, T. M., & Collins, R. E. (1995). *Vacuum glazing—a new component for insulating windows*. Solar Energy, 54(4), 317–323.

[11] NOAA National Centers for Environmental Information, "Climate Normals for Phoenix, AZ," (n.d.). Available: https://www.ncei.noaa.gov

[12] A. R. Gentle and G. B. Smith, "Radiative heat pumping from the Earth using surface phonon polaritons," *Adv. Sci.* **2**(3), 1500119 (2015).

[13] L. Zhou, H. Song, J. Liang, M. Singer, M. Zhou, E. Stegenburgs, N. Zhang, C. Xu, T. Ng, Z. Yu, B. Ooi, and Q. Gan, "A polydimethylsiloxane-coated metal structure for all-day radiative cooling," *Nat. Sustain.* **2**(8), 718–724 (2019).

[14] M. Elkabbash, "Radiative cooling with angular shields: mitigating atmospheric radiation and parasitic heating," *arXiv preprint arXiv:2208.03797* (2022).

[15] G. W. Petty, *A First Course in Atmospheric Radiation*, 2nd ed. (Sundog Publishing, Madison, WI, 2006).